System identification of a cable-stayed bridge using vibration responses measured by a wireless sensor network

Jeong-Tae Kim[*1], Duc-Duy Ho[2], Khac-Duy Nguyen[1], Dong-Soo Hong[1],
Sung Woo Shin[3], Chung-Bang Yun[4] and Masanobu Shinozuka[5]

[1]*Department of Ocean Engineering, Pukyong National University, Busan, Korea*
[2] *Faculty of Civil Engineering, Ho Chi Minh City University of Technology, Ho Chi Minh City, Vietnam*
[3]*Department of Safety Engineering, Pukyong National University, Busan, Korea*
[4]*School of Urban and Environmental Engineering, UNIST, Ulsan, Korea*
[5]*Department of Civil and Environmental Engineering, Univ. of California, Irvine, USA*

Abstract. In this paper, system identification of a cable-stayed bridge in Korea, the Hwamyung Bridge, is performed using vibration responses measured by a wireless sensor system. First, an acceleration based-wireless sensor system is employed for the structural health monitoring of the bridge, and wireless sensor nodes are deployed on a deck, a pylon and several selected cables. Second, modal parameters of the bridge are obtained both from measured vibration responses and finite element (FE) analysis. Frequency domain decomposition and stochastic subspace identification methods are used to obtain the modal parameters from the measured vibration responses. The FE model of the bridge is established using commercial FE software package. Third, structural properties of the bridge are updated using a modal sensitivity-based method. The updating work improves the accuracy of the FE model so that structural behaviors of the bridge can be represented better using the updated FE model. Finally, cable forces of the selected cables are also identified and compared with both design and lift-off test values.

1. Introduction

Since a large cable-stayed bridge represents the potential socio-economic and the cultural symbol of the country, severe malfunction or failure of the bridge can be catastrophic. For a cable-stayed bridge, critical damage may be occurred in main structural components such as deck, cable, and pylon due to stiffness-loss, crack growth, concrete degradation, etc. For example, critical damage in cable-anchorage subsystems includes cable force loss, anchorage damage, and anchorage force loss. Eventually the damage may lead to local or global failure of the bridge system. To avoid the above-mentioned situations, therefore, the cable-stayed bridge must be secured by a suitable SHM system that can identify the occurrence of the damage and assess the location and severity of the damage in a timely manner.

∗Corresponding author, Professor, E-mail: idis@pknu.ac.kr

Since a cable-stayed bridge is a composite and complicated structure, a numerical model of the bridge becomes very important for the damage identification and the safety assessment of the bridge. Also, the identification of tension forces of stay cables can additionally play a role in the damage detection of the bridge (Hua *et al*. 2009). An accurate FE model and frequent evaluations of cable forces may provide a good result of structural damage assessment of a cable-stay bridge. However, it is not easy to construct accurate numerical models of existing cable-stayed bridges due to many uncertainties in model parameters. For example, Cho *et al*. (2010) compared the natural frequencies of the 2nd Jindo Bridge, which is one of famous cable-stayed bridges in Korea, and found large difference (up to 16%) between the natural frequencies of its numerical model and those from the ambient vibration test.

Over the past decades, many researchers have proposed the model updating methods based on vibration characteristics of a structure to improve system identification for the damage detection and assessment (Friswell and Mottershead 1995, Kim and Stubbs 1995, Stubbs and Kim 1996, Zhang *et al*. 2000, Jaishi and Ren 2005, Yang and Chen 2009, Ho *et al*. 2012a). Among those methods, eigenvalue sensitivity-based model updating algorithms have been popularly applied to construct the baseline numerical models of various types of bridges (Brownjohn *et al*. 2001, Wu and Li 2004). However, the application of model updating on cable-stayed bridges has been rarely reported. Zhang *et al*. (2000) updated the finite element (FE) model of the Kap Shui Mun Bridge located in Hong Kong using the eigenvalue sensitivity-based model updating algorithm. Using this algorithm, the differences between the natural frequencies of the FE model and those of the real bridge were reduced from 28% to under 11%. Also, Brownjohn and Xia (2000) updated the initial FE model of the Safti Link cable-stayed bridge in Singapore using the eigenvalue sensitivity-based model updating algorithm. However, the updated FE model still had the large natural frequency difference by about 9%.

This study performs the system identification of a real scale cable-stayed bridge (the Hwamyung Bridge located in Busan, Korea) based on the ambient vibration responses measured by a wireless sensor network. Acceleration responses of a deck, a pylon and several selected cables of the bridge are measured by Imote2-platformed wireless sensor nodes. From the measurement data, modal properties of the deck and the pylon are extracted using frequency domain decomposition and stochastic subspace identification methods. An FE model of the bridge is established based on the design specification of the bridge and the field observation. In order to improve the accuracy of the FE model, a modal sensitivity based system identification algorithm is applied and its effectiveness is discussed. Finally, to update tension forces of the selected cables in the Hwamyung Bridge, cable tension forces are also identified using a frequency-based cable force model and the measured vibration responses. Identified cable tension forces are compared with design and lift-off test values.
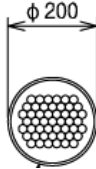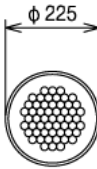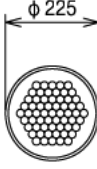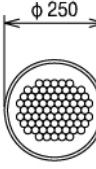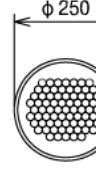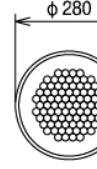

2. Wireless SHM system on the Hwamyung Bridge

2.1 Description of the Hwamyung Bridge

The Hwamyung Bridge is a cable-stayed bridge connecting Busan and Gimhae across the Nakdong river in Korea as shown in Fig. 1. The bridge has been constructed by Hyundai Engineering & Construction Co. from December 2004 to June 2011. It is the longest cable-stayed bridge with prestressed concrete box girder in Korea. As shown in Fig. 2, the bridge consists of

three spans including a 270 m long mid span and two 115 m long side spans. The vertical clearance of the bridge is about 14.7 m. The width of the bridge is 27.8 m, and the heights of the two pylons from the deck level are 65 m. The bridge has total 72 multi-strand type stay cables (18 stay cables at one side of each pylon). The specifications of the cable groups are listed in Table 1. There are six different cable groups (i.e., 49H, 55H, 61H, 73H, 75H and 85H) depending on the number of strands. All the cables are covered by high-density polyethylene (HDPE) ducts with different diameters as 200 mm, 225 mm, 250 mm and 280 mm depending on cable sizes. More detailed information of the bridge can be found in Ho *et al*. (2012b).

Table 1 Specifications of cables in the Hwamyung Bridge

Anchorage type	49H	55H	61H	73H	75H	85H
Strand Num.	49	55	61	73	75	85
Cable cross section	φ 200	φ 225	φ 225	φ 250	φ 250	φ 280
Nominal area (mm^2)	7350	8250	9150	10950	11250	12750
Moment of inertial (mm^4)	4.3×10^6	5.42×10^6	6.66×10^6	9.54×10^6	1.01×10^7	1.29×10^7
Tensile strength (kN)	13671	15345	17019	20367	30925	23715
Elastic modulus (GPa)	195	195	195	195	195	195
Unit mass (kg/m)	67.54	76.34	84.14	101.0	103.6	118.35

2.2 Deployment of smart sensor system

In this study, the Imote2-based sensor boards, SHM-A and SHM-H developed by Rice *et al*. (2010) and Jo *et al*. (2010), respectively, were selected to build a vibration-based SHM system in the Hwamyung Bridge. The SHM-A sensor board employs the tri-axial LIS344ALH accelerometer which has an input range of ± 2g, a sensitivity of 0.66 V/g and an output noise of $50\ \mu g / \sqrt{Hz}$. Meanwhile, the SHM-H sensor board employs the SD1221L-002 accelerometer for a high-sensitivity channel which has an input range of ± 2g, a sensitivity of 2 V/g and an output

noise of 5 $\mu g/\sqrt{Hz}$. Also, the 4-channel 16-bit high resolution ADC with digital anti-aliasing filter (QF4A512) is adopted into both the sensor boards. With the adoption of the digital filters, the sensor boards provide user-selectable sampling rates and cut-off frequencies that can meet a wide range of applications for civil infrastructure monitoring.
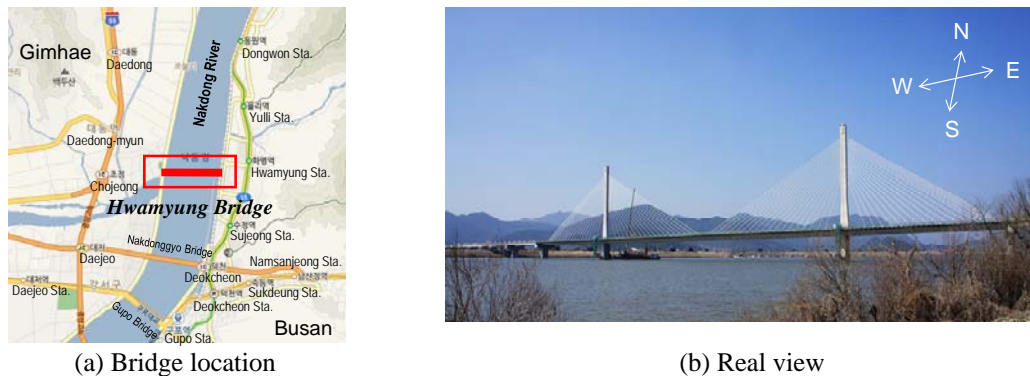

(a) Bridge location

(b) Real view

Fig. 1 On-site view of the Hwamyung Bridge
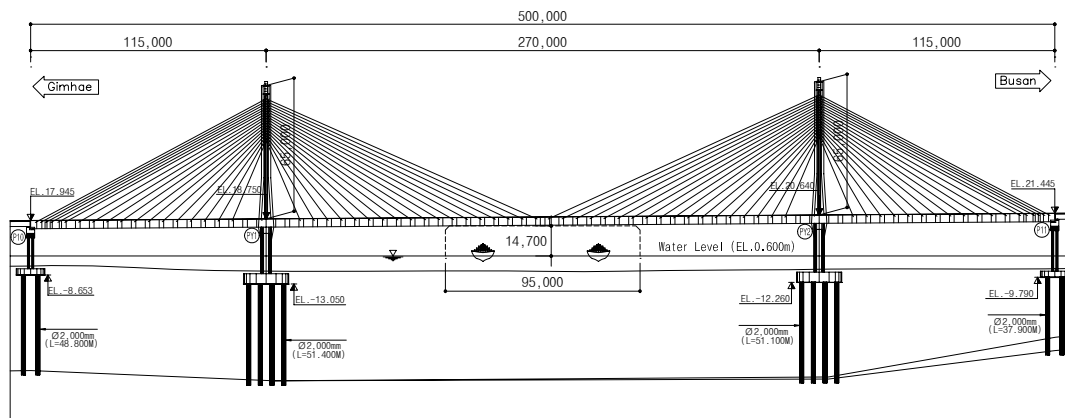
Fig. 2 Geometry of the Hwamyung Bridge

In order to measure vibration response of the Hwamyung Bridge, total eleven Imote2-platformed smart sensor nodes and one gateway node were installed on the bridge. Figure 3 shows the layout of sensor deployment on the bridge, including 6 Imote2/SHM-H nodes on the deck and the west pylon, and 5 Imote2/SHM-A nodes on 5 selected cables. For each sensor node (i.e., Imote2/SHM-H or Imote2/SHM-A), accelerations in the x-, y-, and z-directions were measured using the tri-axial accelerometer. All the sensor nodes and the gateway node were placed

in plastic boxes which have waterproof rubber gaskets to prevent the nodes from sun-heating, absorbent and other malfunctions caused by harsh environmental conditions such as rain, wind and dust at the site. The base station consisted of a PC, a gateway node and a commercial broadband (T-login) modem to connect the PC to the internet. The sensor nodes were powered by Li-ion polymer rechargeable batteries. Solar panels were mounted on the sensor boxes to harvest the solar energy and recharge the batteries. By implemented with *AutoMonitor* component, the sensor system was activated every two hours and measured the accelerations in 10 minutes with a sampling rate of 25 Hz. More detailed information of the sensor deployment can be found in Ho (2012) and Ho *et al.* (2012b)

Fig. 4 shows examples of acceleration responses and the corresponding power spectral densities of the pylon, the deck and the cables (i.e., sensor nodes P1, D2 and C4) under normal condition (without vehicle traffic on the bridge). Nevertheless of this low excitation condition, the maximum acceleration amplitudes are relatively high, such as 0.6 mg for pylon P1, 0.3 mg for deck D2, and 14 mg for cable C4. Also, natural frequencies of the bridge components can be well determined, which guarantees a reliable modal identification. Note that there are unexpected periodic peaks (i.e., 0.8 Hz, 1.6 Hz) in the frequency responses as shown in Fig. 4. It has been reported that these noise peaks can be caused by the power supply issue of the SHM-H sensor board (Jo *et al.* 2010).

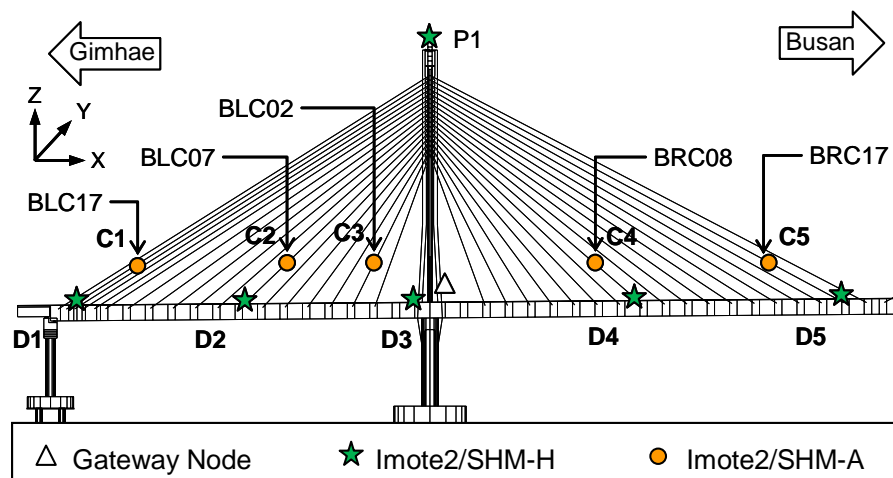Fig. 3 Field sensor layout on the Hwamyung Bridge: 33 acceleration channels

3. Modal parameter identification

3.1 Numerical modal analysis

In order to calculate modal parameters, an FE model of the Hwamyung Bridge was established using SAP2000 as shown in Fig. 5. The two pylons and the main girder were modeled by frame elements with dimensions as same as the design values. The stay cables were modeled by cable

elements whose equivalent circular cross sections are the same as the designed nominal areas of the cables. Since the stay cables are modeled using cable elements, nonlinear stiffness of the cables due to the post-tensioning forces can be taken into account.

(a) Top pylon P1: Acceleration

(b) Top pylon P1: PSD of acceleration

(c) Deck D2: Acceleration

(d) Deck D2: PSD of acceleration

(e) Cable C4: Acceleration
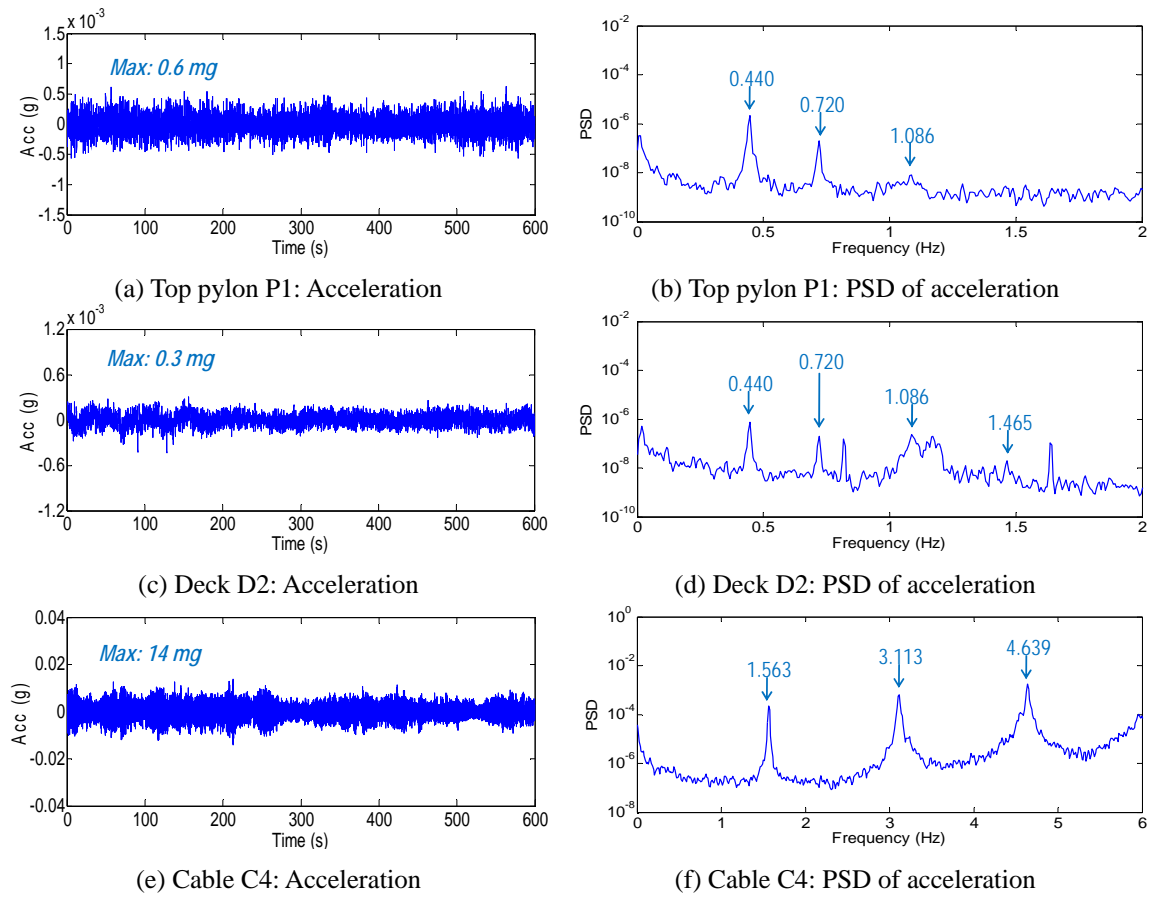
(f) Cable C4: PSD of acceleration

Fig. 4 Acceleration responses and power spectral densities under normal condition

The material of the girder and the two pylons was defined as concrete with the following properties: Young's modulus of 28.6 GPa, Poisson's ratio of 0.2, and mass density of 2500 kg/m^3. The material of the cables was defined as steel with Young's modulus of 195 GPa, Poisson's ratio of 0.3, and mass density of 7850 kg/m^3. For the boundary conditions, the supports of the two pylons and the two girder ends were modeled by three directional springs as shown in Fig. 5. Since the stiffness values of the supporting springs depend on the foundation conditions which is beyond the scope of this study, they were assumed as $k_{d-x} = 10^6$ N/m, $k_{d-y} = 5 \times 10^7$ N/m, $k_{d-z} = 10^9$ N/m for the deck supports, and $k_{p-x} = 10^{10}$ N/m, $k_{p-y} = 10^{10}$ N/m, $k_{p-z} = 10^{10}$ N/m for the pylon supports. To complete the FE model, the tension force of each stay cable in the model was assigned using the tension force measured from lift-off test. It should be noted that the lift off test was carried out on December 2010.
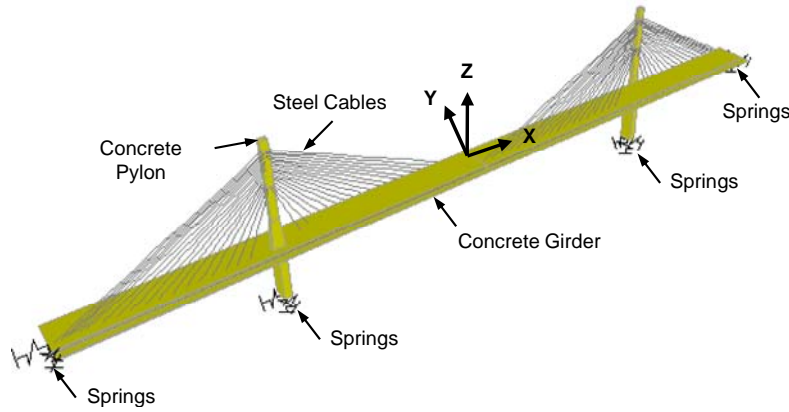
Fig. 5 FE model of the Hwamyung Bridge

3.2 Experimental modal analysis

The modal parameters (natural frequency, mode shape, and damping ratio) can be obtained by modal identification methods such as frequency domain decomposition (FDD) method and stochastic subspace identification (SSI) method. In this study, both methods were employed to extract modal parameters of the Hwamyung Bridge.

Modal parameter extraction by FDD method

The FDD method utilizes the singular value decomposition (SVD) of the PSD matrix, $\mathbf{S}_{xx}(\omega)$, to estimate natural frequencies and mode shapes as follows (Brincker *et al*. 2001)

$$\mathbf{S}_{xx}(\omega) = \mathbf{U}(\omega)^T \mathbf{\Sigma}(\omega) \mathbf{V}(\omega) \tag{1}$$

where $\sum(\omega)$ is the diagonal matrix containing the singular values of the PSD matrix; and $\mathbf{U}(\omega)$ and $\mathbf{V}(\omega)$ are the unitary matrices. The natural frequencies are determined from the peak frequencies of the first singular values. The mode shapes are determined from the correspondent column vectors of $\mathbf{U}(\omega)$ at the natural frequencies.

Damping ratios can be found by constructing the corresponding singular degree of freedom (SDOF) system. This SDOF is identified as part of the first singular values around the natural frequency. The SDOF is taken back to single time domain by an inverse fast Fourier transform (IFFT). Then, damping ratios are estimated using the logarithmic decrement of the single time domain.

The first singular values of the deck's and the pylons' responses of the Hwamyung Bridge are plotted in Fig. 6. Four vertical modes (V1, V2, V4, and V6) and three lateral modes (L1, L2, and L3) are identified from the singular values. The corresponding natural frequencies are listed in

Table 2. The modal damping ratios were also extracted by the FDD method as summarized in Table 5.

(a) Vertical response

(b) Lateral responses
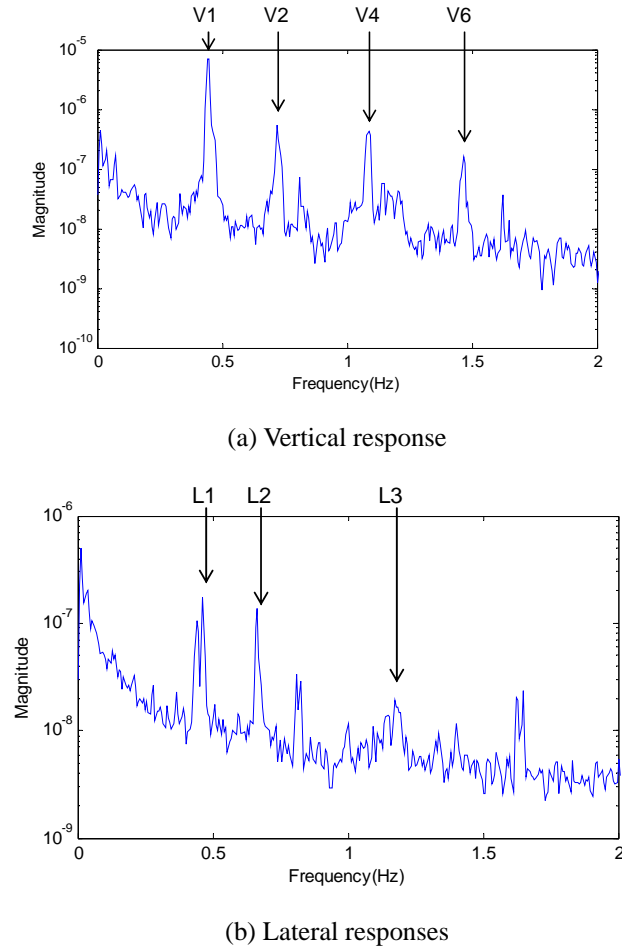
Fig. 6 FDD method: Singular values for deck's and pylons' responses

Modal parameter extraction by SSI method

The SSI method utilizes the singular value decomposition (SVD) of a block Hankel matrix with cross correlation matrix of responses as follows (Overschee and De Moor 1996)

$$\mathbf{H} = \begin{bmatrix} \mathbf{U_1} & \mathbf{U_2} \end{bmatrix} \begin{bmatrix} \mathbf{\Sigma_1} & 0 \\ 0 & 0 \end{bmatrix} \begin{bmatrix} \mathbf{V}_1^T \\ \mathbf{V}_2^T \end{bmatrix} \approx \mathbf{U_1}\mathbf{\Sigma_1}\mathbf{V}_1^T$$

(2)

where $\mathbf{H}$ is the Hankel matrix; $\mathbf{U}, \mathbf{V}$ are the unitary matrices; and Σ_1 is the singular value matrix. The modal parameters can be identified from a system matrix which is determined from

the SVD algorithm. A stabilization chart is used to find a suitable system order with the criteria which classify a mode as stable mode, unstable mode, and noise mode (Yi and Yun 2004). Once the stable modes are detected, damping ratio (ξ_i) of the ith mode is identified from the eigenvalue (λ_i) as follows

$$\xi_i = \frac{-\mathrm{Re}(\lambda_i)}{|\lambda_i|} \tag{3}$$

Examples of stabilization charts for the vertical and transverse responses of the Hwamyung Bridge are shown in Fig. 7. It is seen that the first six vertical bending modes (V1-V6) and three transverse bending modes (L1-L3) are very stable modes and thus modal parameters for those modes are extracted. The natural frequencies and the modal damping ratios extracted by the SSI method are listed in Tables 2 and 3, respectively. It is found that the SSI method clearly identifies modes V3 and V5 which were not able to be obtained by the FDD method. It should be noted that the SSI process is time-consuming but the results are generally more accurate than the FDD method (Yi and Yun 2004). In order to obtain better results from the FDD method, a longer measuring time may be required. However, in this study, the natural frequencies and the damping ratios for the modes identified by the FDD method are well agreed with those by the SSI method as shown in Tables 2 and 3. This good agreement provides high reliability on modal extraction using vibration responses by the wireless sensor system. Since the SSI method showed the better performance on modal extraction than the FDD method, the results by the SSI method are considered as the precise modal behavior of the bridge.

Table 2 Natural frequencies (Hz): initial FE model vs experiment

	Vertical modes						Lateral modes		
	V1	V2	V3	V4	V5	V6	L1	L2	L3
Initial FE model	0.466	0.681	1.082	1.158	1.275	1.564	0.443	0.669	1.136
Experiment (FDD)	0.446	0.720	-	1.087	-	1.465	0.464	0.665	1.172
Experiment (SSI)	0.444	0.720	1.028	1.084	1.171	1.462	0.454	0.666	1.169
Difference (%): FEM/FDD	4.5	5.4	-	6.5	-	6.8	4.5	0.6	3.1
Difference (%): FEM/SSI	4.9	5.4	5.3	6.8	8.8	7.0	2.4	0.4	2.8

* Symbol L indicates lateral mode, symbol V indicates vertical mode.

Table 3 Damping ratios extracted from experimental test

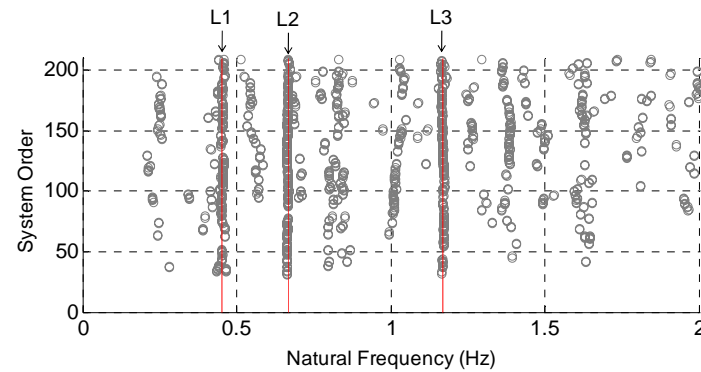|	Vertical modes						Lateral modes		
	V1	V2	V3	V4	V5	V6	L1	L2	L3
FDD	0.004	0.011	-	0.005	-	0.005	0.017	0.013	0.026
SSI	0.004	0.009	0.025	0.006	0.028	0.008	0.012	0.011	0.026
Difference (%)	0	22.2	-	16.7	-	37.5	41.7	18.2	0
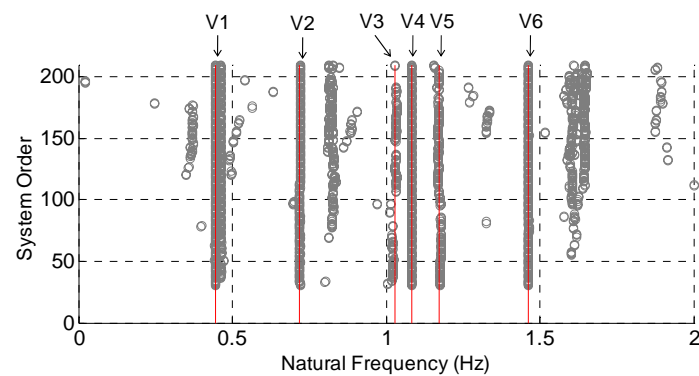
(a) Vertical response

(b) Lateral responses

Fig. 7 SSI method: Stabilization charts for deck's and pylons' responses

Fig. 8 shows the calculated and identified natural frequencies and mode shapes of the Hwamyung Bridge. The calculated modal parameters were obtained from the initial FE model, while the identified parameters were obtained by the SSI method. As shown in Fig. 8, the mode shapes identified by the SSI method match well with those of the initial FE model. However, as listed in Table 2, the differences between the natural frequencies from the FE analysis and those

from the experiment are ranged from 0.4% to 8.8%. Therefore, the initial FE model needs to be fine-tuned appropriately to represent better the behaviors of the bridge.

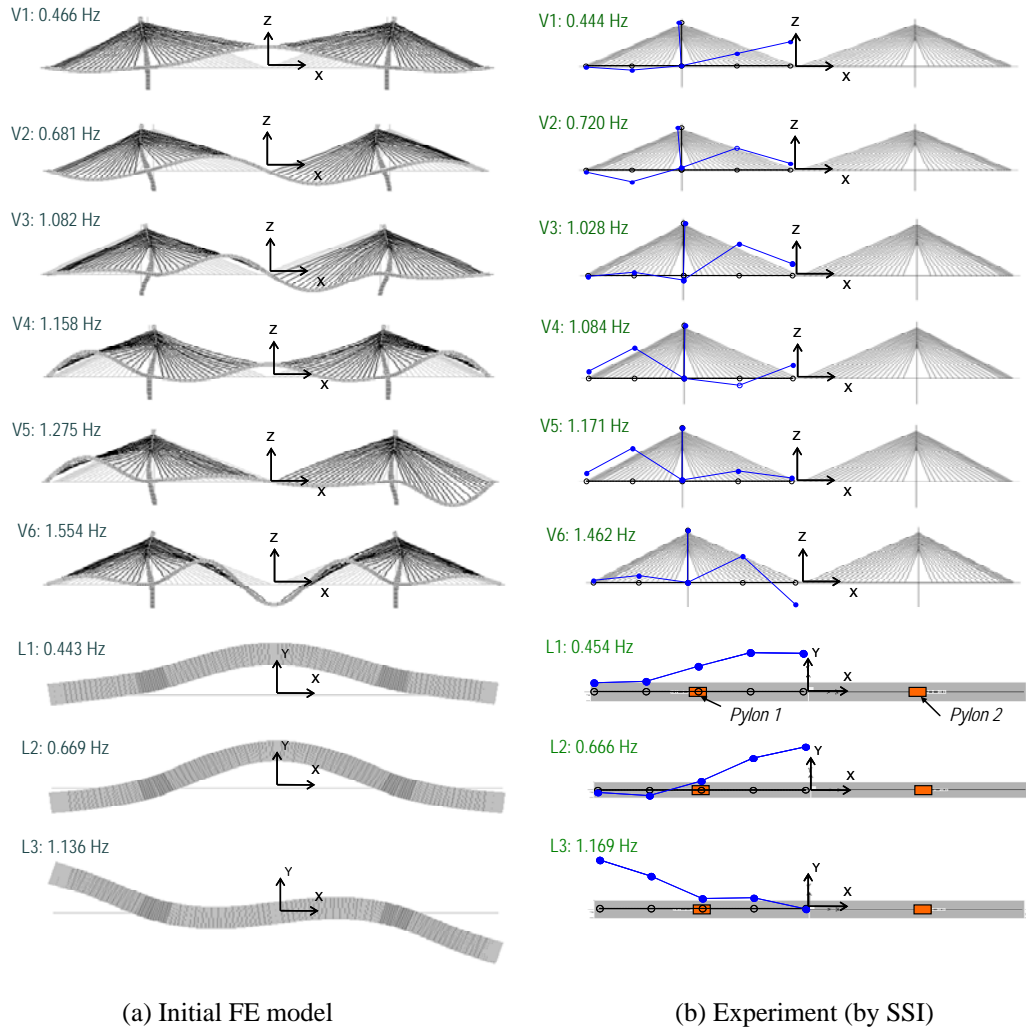|	
(a) Initial FE model	(b) Experiment (by SSI)

Fig. 8 Modal parameters: initial FE model vs experiment

4. System identification of deck and pylon

4.1 Modal strain energy-based system identification method

In order to perform the structural integrity assessment which is the last step of SHM, a baseline

model of the Hwamyung Bridge should be identified. Then, the identified baseline model can play a role of the reference structure to make diagnosis on the target bridge. For this purpose, structural parameters of the Hwamyung Bridge are updated using a modal strain energy-based system identification method. Modal strain energy is one of the damage sensitive features using mode shape and modal stiffness concepts. It has been shown that the modal strain energy is more sensitive for structural parameter identification than the mode shape (Stubbs *et al*. 1992, Kim and Stubbs 1995, Doebling *et al*. 1998, Kim *et al*. 2006). The modal strain energy for the ith mode and j^{th} member (i.e., modal sensitivity F_{ij}) is given by (Stubbs and Kim 1995)

$$F_{ij} = \frac{\Phi_i^T \mathbf{C}_j \Phi_i}{\Phi_i^T \mathbf{C}\, \Phi_i} \tag{4}$$

where Φ_i is the ith mode shape vector, $\mathbf{C}$ is the system stiffness matrix, and $\mathbf{C}_j$ is the contribution of the jth member to the system stiffness.

Based on the concept of the modal strain energy, Stubbs and Kim (1996) proposed a system identification method to identify a realistic theoretical model of a structure. Suppose k_j^* is an unknown stiffness of the jth member of a structure for which M measured eigenvalues are known. Also, suppose k_j is a known stiffness of the jth member of a finite element (FE) model for which the corresponding set of M computed eigenvalues are known. Then, relative to the FE model, the fractional structural parameter change of the jth member, $\alpha_j \geq -1$, and the structural parameters are related according to the following equation

$$k_j^* = k_j \left(1 + \alpha_j\right) \tag{5}$$

The dimensionless modal sensitivity, F_{ij}, of the ith eigenvalue ω_i^2 with respect to the jth structural stiffness k_j is defined as follows

$$F_{ij} = \frac{\delta \omega_i^2}{\delta k_j} \frac{k_j}{\omega_i^2} \tag{6}$$

where δk_j is the first order perturbation of k_j which produces the variation in eigenvalue $\delta \omega_i^2$. The fractional structural parameter change of *NE* members may be obtained using the following equation

$$\{\alpha\} = [\mathbf{F}]^{-1} \{Z\} \tag{7}$$

where $\{\alpha\}$ is a $NE \times 1$ matrix containing the fractional changes in structural parameters between the FE model and the target structure; $\{Z\}$ is a $M \times 1$ matrix containing the fractional changes in eigenvalues between two systems; and $|\mathbf{F}|$ is a $M \times NE$ sensitivity matrix. To identify the completeness of the FE model updating process, the convergence criterion between the measured and analytical eigenvalues is set as follows

$$\left| Z_i \right| = \left| \frac{\omega_{i,m}^2 - \omega_{i,a}^2}{\omega_{i,a}^2} \right| \leq tolerance$$

(8)

where $\omega_{i,m}^2$ and $\omega_{i,a}^2$ are the ith eigenvalues of the measured target structure and the analytical model, respectively.

Using the above theory as a basis, the modal strain energy-based system identification method is implemented as the following three steps: 1) Calculate the sensitivity of stiffness parameters by Eq. (6); 2) Fine-tune the FE model by solving Eq. (7) to estimate changes in stiffness parameters and then solving Eq. (5) to update the stiffness parameters of the FE model; and 3) Repeat the whole procedure until Eq. (8) is satisfied.

4.2 Identification of structural parameters

Model-updating Parameters

Choosing appropriate structural parameters is an important step in the FE model-updating procedure. All parameters related to structural geometries, material properties, and boundary conditions can be potential choices for adjustment in the model-updating procedure. The availability of as-built documents of structural information and the sensitivities of structural parameters to structural responses should be considered to select appropriate model-updating parameters. Physically, the structural parameters which are uncertain in the model due to the lack of information on structural properties should be selected. Also, the structural parameters which are relatively sensitive to vibration responses should be selected. For the Hwamyung Bridge, nine potential groups of model-updating parameters were selected as follows:

(1) stiffness of deck $(EI)_d$;

(2) stiffness of upper-pylons $(EI)_{u-p}$;

(3) stiffness of lower-pylons $(EI)_{l-p}$;

(4) stiffness of X-directional deck support springs $(k)_{d-x}$;

(5) stiffness of Y-directional deck support springs $(k)_{d-y}$;

(6) stiffness of Z-directional deck support springs $(k)_{d-z}$;

(7) stiffness of X-directional pylon support springs $(k)_{p-x}$;

(8) stiffness of Y-directional pylon support springs $(k)_{p-y}$; and

(9) stiffness of Z-directional pylon support springs $(k)_{p-z}$.

Then, the eigenvalue sensitivities of the nine groups of model-updating parameters to the nine

eigen-frequencies were calculated by Eq. (6), as listed in Table 4 and also shown in Fig. 9. Note that the stiffness of the deck and the pylons were constrained within 10% since the initial values of these parameters were assumed as same as the design specifications. Meanwhile, the stiffness parameters of the support springs were unconstrained since the foundation conditions are not investigated in this study.

From the sensitivity analysis, the stiffness of the deck was found to be the most sensitive parameter to both the vertical and lateral modes. The stiffness of the pylons was the comparably sensitive parameters. The stiffness of the support springs were found to be the least sensitive parameters, as shown in Fig. 9. Due to the availability of the nine modes including six vertical modes and the three lateral modes, one model-updating phase was chosen to update the nine model-updating parameters.

Table 4 Eigenvalue sensitivities of model-updating parameters

Mode	Eigenvalue sensitivity								
	$(EI)_d$	$(EI)_{u-p}$	$(EI)_{l-p}$	$(k)_{d-x}$	$(k)_{d-y}$	$(k)_{d-z}$	$(k)_{p-x}$	$(k)_{p-y}$	$(k)_{p-z}$
V1	3.9E-1	3.8E-2	7.6E-2	4.9E-5	2.1E-12	1.1E-2	3.7E-3	3.6E-12	5.4E-3
V2	4.0E-1	9.3E-2	3.3E-1	1.3E-3	3.4E-12	8.0E-3	7.8E-3	4.7E-12	6.5E-4
V3	4.0E-1	6.7E-2	3.2E-1	9.1E-4	-1.1E-12	8.2E-5	2.6E-2	0.0E+0	6.9E-3
V4	5.2E-1	4.9E-2	6.4E-2	1.3E-5	-8.6E-13	1.3E-2	3.6E-3	-1.7E-13	1.1E-2
V5	5.0E-1	3.1E-2	1.2E-1	3.0E-4	-2.2E-12	1.3E-2	1.2E-2	-1.1E-12	1.6E-2
V6	6.5E-1	3.7E-2	2.9E-2	1.8E-5	-3.1E-12	1.4E-3	1.3E-3	-2.0E-11	1.6E-2
L1	8.0E-3	9.3E-1	1.7E-1	-1.0E-7	6.6E-5	-3.9E-5	-2.4E-5	1.7E-3	-3.2E-5
L2	6.3E-1	3.5E-2	1.6E-1	5.6E-6	2.1E-1	2.6E-5	1.4E-4	7.1E-3	2.3E-5
L3	2.3E-1	1.6E-2	1.1E-1	2.9E-6	6.6E-1	3.0E-6	1.1E-5	7.1E-3	2.5E-6

Updated structural parameters

After selecting the dynamic responses and the structural parameters, model updating process was carried out using Eqs. (5)-(8). The structural parameters of the bridge can be identified by matching the modal parameters of the FE model and those obtained from experimental data. Table 5 shows the natural frequencies of the FE model during updating iterations. Fig. 10 shows the errors of the natural frequencies of the updated model during the iterations, with compared to the experimental natural frequencies. The errors converged to 0.0-4.9 (%) after the final iteration. Note that the maximum difference between the numerical and the experimental values reduced from 8.8% to 4.9% after the updating process. It is also found that the updated fundamental natural frequency (i.e., mode V1) matches very well with the experimental value (1.4% difference).
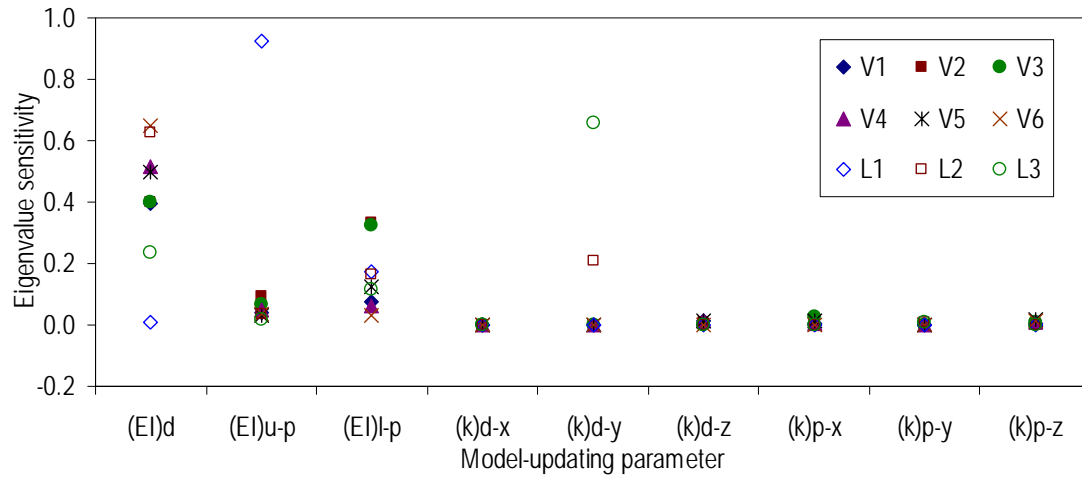
Fig. 9 Comparison of eigenvalue sensitivities of model-updating parameters

The relative changes in the model-updating parameters of the FE model during the updating process are shown in Fig. 11. It is seen that the changes were large at the earlier iterations and converged to the unity at the later iterations. It is found that the stiffness of the deck and the pylons converged more rapidly to the unity than those of the supports. This is reasonable since the stiffness of the deck and the pylons are more sensitive to the change in eigenvalues than those of the supports as described by the sensitivity analysis in previous section. The identified structural parameters (i.e., updated parameters) are listed in Table 6. Compared to the initial parameters of the initial FE model, the stiffness of the deck was decreased by 5.1%. On the other hand, the stiffness of the upper-pylons and the stiffness of the lower-pylons were increased by 6.7% and 10%, respectively. The stiffness of the support springs, which were assumed as uncertain parameters, changed significantly (up to 620% for $(k)_{d-z}$).

Although the FE model was updated successfully with small differences in natural frequencies with respect to the experiment, several issues on the model updating results should be discussed. First, the convergence error indicates that the updated model does not represent exactly the real behaviors of the bridge. The convergence error can be reduced using a fewer modes in model updating process. However, in this case, the damage assessment may become less reliable. A better way to reduce the convergence error is to increase model-updating parameters in the updating process. Second, the updating results would be more reliable if the natural frequencies and the mode shapes are considered simultaneously in the model updating process. Third, the error of the updated model is about 4.9% with respect to the natural frequencies. The higher accuracy may be required to assess the current condition of the bridge more reliably.

Table 5 Natural frequencies of FE model during model update

| Mode	Initial freqs. (Hz)	Updated frequencies (Hz) at each iteration												Target freqs. (Hz)
		1	2	3	4	5	6	7	8	9	10	11	12	
V1	0.466	0.464	0.463	0.458	0.456	0.455	0.453	0.451	0.450	0.450	0.450	0.450	0.450	0.444
V2	0.681	0.684	0.686	0.682	0.681	0.682	0.683	0.684	0.684	0.684	0.685	0.685	0.685	0.720
V3	1.082	1.083	1.085	1.073	1.070	1.062	1.045	1.022	1.019	1.020	1.024	1.025	1.027	1.028
V4	1.158	1.151	1.146	1.128	1.117	1.107	1.089	1.070	1.066	1.064	1.067	1.067	1.068	1.084
V5	1.275	1.266	1.262	1.239	1.230	1.223	1.211	1.199	1.200	1.202	1.205	1.206	1.207	1.171
V6	1.564	1.555	1.543	1.517	1.501	1.480	1.450	1.425	1.423	1.423	1.428	1.429	1.431	1.462
L1	0.443	0.443	0.454	0.460	0.462	0.464	0.464	0.463	0.458	0.461	0.457	0.456	0.455	0.454
L2	0.669	0.674	0.673	0.666	0.664	0.661	0.657	0.656	0.653	0.653	0.653	0.653	0.653	0.666
L3	1.136	1.167	1.174	1.169	1.168	1.168	1.167	1.166	1.169	1.169	1.169	1.169	1.169	1.169
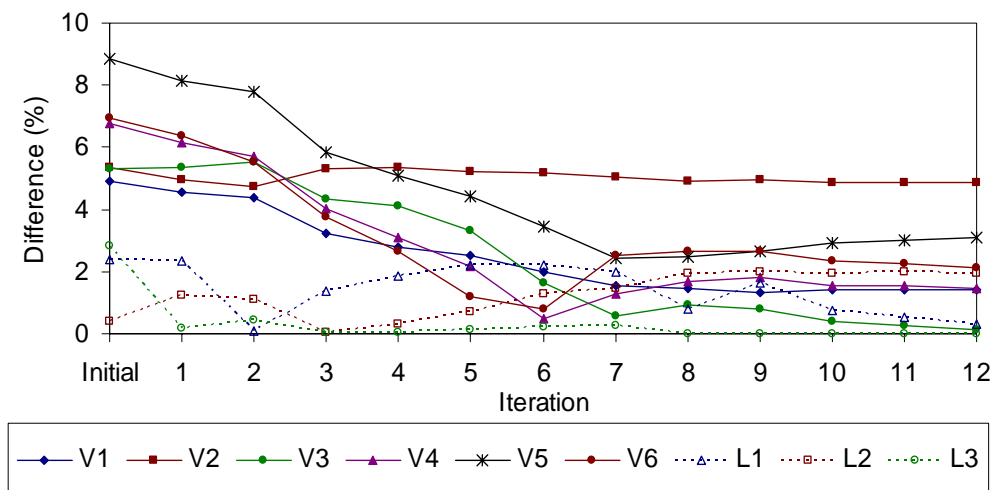
Fig. 10 Convergences of natural frequencies between FE model and experiment
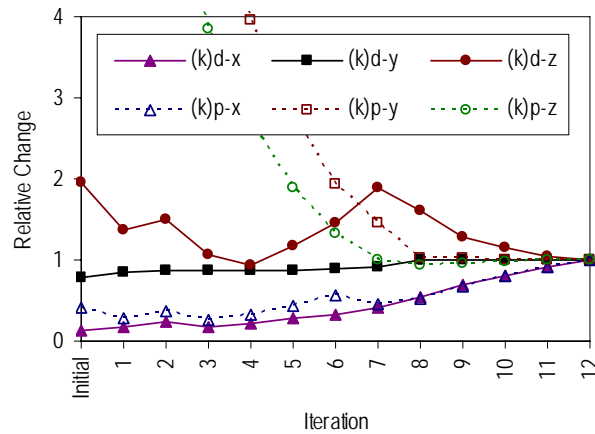
Table 6 Model-updating parameters: initial value versus updated value

Parameter	$(EI)_d$	$(EI)_{u-p}$	$(EI)_{l-p}$	$(k)_{d-x}$	$(k)_{d-y}$	$(k)_{d-z}$	$(k)_{p-x}$	$(k)_{p-y}$	$(k)_{p-z}$
	(Nm^2)	(Nm^2)	(Nm^2)	(N/m)	(N/m)	(N/m)	(N/m)	(N/m)	(N/m)
Initial value	9.9E+10	1.7E+11	5.0E+11	1.0E+6	5.0E+7	1.0E+9	1.0E+10	1.0E+10	1.0E+10
Updated value	9.4E+10	1.8E+11	5.5E+11	7.2E+6	6.4E+7	5.1E+8	2.5E+10	9.1E+8	8.9E+8
Change (%)	-5.1	6.7	10.0	620.0	28.0	-49.0	150.0	-90.9	-91.1
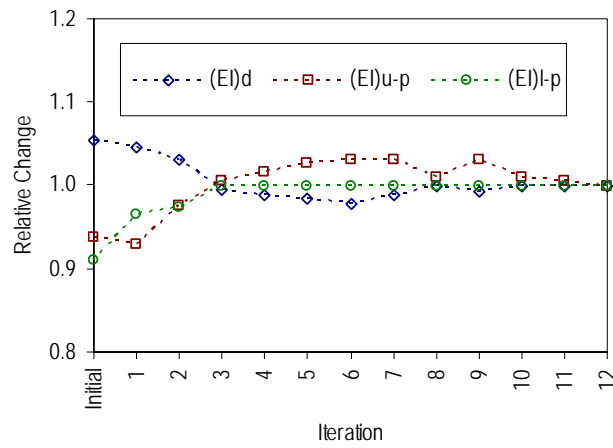
(a) Stiffness of deck and pylons

(b) Stiffness of support springs

Fig. 11 Relative change in model-updating parameters of FE model

5. Cable force estimation

In cable-stayed bridge, stay cables are essential components since they carry most of the loads of a deck and transfer those loads to pylons. Therefore, sufficient and accurate information of cable parameters is required to ensure the serviceability of the bridge. These parameters can be classified as material properties (e.g., elastic modulus, mass density), geometries (e.g., cross section, length) and cable force. For the Hwamyung Bridge, the material properties of the cables which are made of steel can be identified reliably from the manufacture's specifications as outlined in Table 1. Also, the lengths of the cables can be easily obtained by determining the locations of two ends of the cables; and cross sections of the cables are maintained as good as the design specification by orienting the cables through anchorage components. The least controllable parameters of the cables would be the tension forces. Normally, the cables are stressed to particular forces according to the design. However, the cable forces can be changed over the time due to the stress relaxation of steel. Therefore, it is necessary to update the tension forces of the cables.

The techniques to estimate cable force are classified into static and vibration-based methods. In the static method, cable force is directly measured by a load cell or a hydraulic jack. In the vibration-based method, cable force is indirectly estimated from measured natural frequencies. In practice, the vibration-based method is more widely used than the static method due to its simplicity in test procedure (Kim and Park 2007). Among available vibration-based methods (Clough and Penzien 1993, Shimada 1995, Zui *et al*. 1996), the method proposed by Zui *et al*. (1996) is selected in this study to estimate the cable forces. The merit of this method is that the effects of both flexural rigidity and cable-sag are considered in the estimation of cable tension force so that the accuracy of the estimation can be greatly improved. For simplification, the cable tension force (*T*) is determined using multiple vibration modes (*NM*) as follow

$$T = \frac{1}{NM}\sum_{n=1}^{NM} T_n \tag{9}$$

and

$$T_n = \frac{4m}{n^2}(f_n L)^2 \left[1 - 2.2n\frac{C}{f_n} - 0.55n\left(\frac{C}{f_n}\right)^2\right]; \quad \xi < 200 \tag{10a}$$

$$T_n = \frac{4m}{n^2}(f_n L)^2 \left[1 - 2.2n\frac{C}{f_n}\right]; \quad \xi \geq 200 \tag{10b}$$

where T_n is the tension force by the nth vibration mode; *m* is the mass of cable per unit length; *L* is the length of cable; f_n is the nth natural frequency; ξ is the parameter determined from cable properties and design conditions, $\xi = \sqrt{(T/EI)} \times L$; $C = \sqrt{(EI/mL^4)}$; and *EI* is the flexural rigidity of cable.

Using the SSI method, the natural frequencies of the five selected cables C1-C5 measured by the wireless sensor nodes are listed in Table 7. The tension forces of the five cables are estimated

using Eqs. (9)-(10). The estimation results are summarized in Table 7 and also shown in Fig. 12 together with the design forces and the lift-off test results. It is found that the vibration-based estimation results are much different from the design forces by about 0.4 - 10.3 (%). On the other hand, relatively smaller difference (about 1.1 - 6.3 (%)) is observed between the estimations and the measures from the lift-off test. It should be noted that the design force can be used as a reference but it does not represent the true cable force. The lift-off test results may represent the true cable tension forces at the time of the test. However, the lift-off test was carried out in December 2010 which was 6 months before the vibration test (June 2011). Hence, the estimated cable tension forces in this study could be considered as the most updated data.

Table 7 Estimated tension forces of cables C1-C5

| Cable | Tpe | Span length (m) | Design force (kN) | Liff-off force (kN) | Natural frequencies (Hz) | | | Estimated Force (kN) | Difference (%) | |
					1st	2nd	3rd		Est/ Design	Est./Lift-off
C1	73H	123.806	7456.3	7583.1	1.139	2.270	3.404	7857.8	5.4	3.6
C2	55H	72.733	4728.4	4856.6	1.741	3.452	5.143	4681.1	1.0	3.6
C3	49H	44.893	4828.0	4625.5	2.912	5.668	8.702	4332.3	10.3	6.3
C4	55H	78.364	4278.9	4336.1	1.559	3.107	4.619	4386.8	2.5	1.2
C5	85H	136.813	9612.4	9550.3	1.053	2.104	3.155	9652.1	0.4	1.1
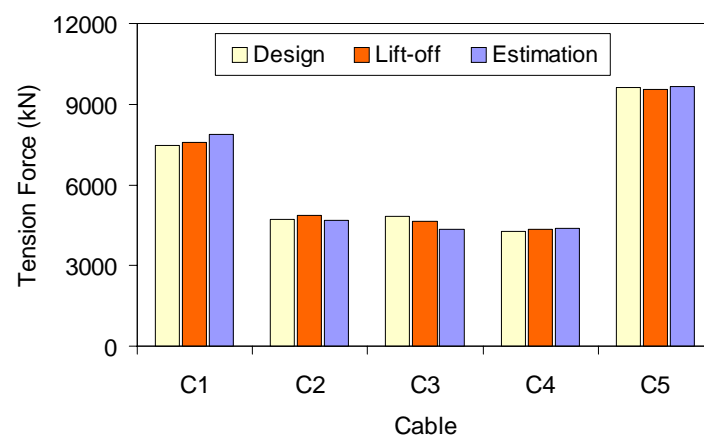
Fig. 12 Cable force estimation: Cables C1-C5

6. Conclusions

This paper presented the system identification of a cable-stayed bridge, the Hwamyung Bridge in Korea, using vibration responses measured by a wireless sensor system. Acceleration based-wireless sensor nodes were deployed on a deck, a pylon and several selected cables for the structural health monitoring of the bridge. Modal parameters of the bridge were extracted from measured vibration responses, and were numerically analyzed by an FE model. Frequency domain decomposition and stochastic subspace identification method were used to obtain the experimental modal parameters. The FE model of the bridge was established using SAP2000 with dimensions, material properties, and boundary conditions obtained from the design specification of the bridge and by the observation. Then, structural properties of the bridge were updated using a modal sensitivity-based method. Cable forces of the selected cables were also identified and compared with both design and lift-off values.

From the system identification results, the following conclusions have been made. Experimental modal parameters of the target bridge were accurately extracted with compared to the numerical modal parameters. A baseline FE model representing structural parameters of the bridge at the test period was successfully estimated. The natural frequencies were well converged within 0.0%-4.9% differences with respect to the experiment. Based on the updating process, structural parameters of the target bridge were also successfully identified. The estimated cable forces showed differences with design values by 0.4 - 10.3 (%) and with the lift-off test values by 1.1 – 6.3 (%) depending on the cables.

This study successfully provided a baseline FE model of the Hwamyung Bridge. The material properties of the deck and the pylons, the boundary conditions, and tension forces of several cables have been updated. The baseline FE model and the current estimated cable forces can be used as references for the assessment of health status of the bridge in the future. This study also demonstrated the feasibility of the modal strain energy-based method on model-updating for a large, complicated, real scale cable-stayed bridge. The future works are remained to monitor tension forces of other cables, and to deploy more sensors over two sides of the bridge to get more sufficient information for damage assessment analysis. Also, longer time history responses should be measured to extract better modal parameters of the bridge.

Acknowledgements

References

Brincker, R., Zhang, L., and Andersen, P. (2001), "Modal identification of output-only systems using frequency domain decomposition", *Smart Mater. Struct.*, **10**, 441-445.
Brownjohn, J.M.W. and Xia, P.Q. (2000), "Dynamic assessment of curved cable-stayed bridge by model

updating", *J. Struct. Eng-ASCE.*, **126**(2), 252-260.

Brownjohn, J.M.W., Xia, P.Q., Hao, H. and Xia, Y. (2001), "Civil structure condition assessment by FE model updating: methodology and case studies", *Finite Elem. Anal. Des.*, **37**, 761-775.

Cho, S., Jo, H., Jang, S., Park, J., Jung, H.J., Yun, C.B., Spencer, B.F. and Seo, J.W. (2010), "Structural health monitoring of a cable-stayed bridge using wireless smart sensor technology: data analyses", *Smart Struct. Syst.*, **36** (5-6), 461-480.

Clough, R.W. and Penzien, J. (1993), *Dynamics of structures*, Second Edition, McGraw-Hill

Doebling, S.W., Farrar, C.R. and Prime, M.B. (1998), "A summary review of vibration-based damage identification methods", *Shock Vib.,* **30**(2), 91-105.

Friswell, M.I. and Mottershead, J.E. (1995), *Finite element model updating in structural dynamics*, Kluwer Academic, Boston.

Ho, D.D. (2012), "Multi-scale smart sensing of vibration and impedance for structural health monitoring of cable-stayed bridge", *Ph.D dissertation*, Pukyong National University, Korea.

Ho, D.D., Kim, J.T., Stubbs, N., and Park, W.S. (2012a), "Prestress-force estimation in PSC girder using modal parameters and system identification", *Advances in Structural Engineering*, **15**(6), 997-1012.

Ho, D.D., Lee, P.Y., Nguyen, K.D., Hong, D.S., Lee, S.Y., Kim, J.T., Shin, S.W., Yun, C.B. and Shinozuka, M. (2012b), "Solar-powered multi-scale sensor node on Imote2 platform for hybrid SHM in cable-stayed bridge", *Smart Struct. Syst.*, **9**(2), 145-164.

Hua, X.G., Ni, Y.Q., Chen, Z.Q. and Ko, J.M. (2009), "Structural damage detection of cable-stayed bridges using changes in cable forces and model updating", *J. Struct. Eng. -ASCE*, **135**(9), 1093-1106.

Jaishi, B. and Ren, W.X. (2005), "Structural finite element model updating using ambient vibration test results", *J. Struct. Eng. -ASCE*, **131**(4), 617-628.

Jo, H., Rice, J.A., Spencer, B.F. and Nagayama, T. (2010), "Development of a high-sensitivity accelerometer board for structural health monitoring", *Proceedings of the SPIE*, San Diego, USA.

Kim, J.T., Na, W.B., Park, J.H. and Hong, D.S. (2006), "Hybrid health monitoring of structural joints using modal parameters and EMI signatures", *Proceedings of the SPIE*, San Diego, USA.

Kim, J.T. and Stubbs, N. (1995), "Model-uncertainty impact and damage-detection accuracy in plate girder", *J. Struct. Eng. - ASCE*, **121**(10), 1409-1417.

Kim, B.H. and Park, T. (2007), "Estimation of cable tension force using the frequency-based system identification method", *J. Sound Vib.*, **304**, 660-676.

Overschee, V.P. and De Moor, B. (1996), *Subspace identification for linear system*, Kluwer Academic Publisher.

Rice, J.A., Mechitov, K., Sim, S.H., Nagayama, T., Jang, S., Kim, R., Spencer, Jr, B.F., Agha, G. and Fujino, Y. (2010), "Flexible smart sensor framework for autonomous structural health monitoring", *Smart Struct. Syst.*, **6**(5-6), 423-438.

Shimada, T. (1995), *A study on the maintenance and management of the tension measurement for the cable of bridge*, Ph.D. Dissertation, Kobe University, Japan.

Stubbs, N. and Kim, J.T. (1996), "Damage localization in structures without baseline modal parameters", *AIAA J.*, **34**(8), 1644-1649.

Stubbs, N., Kim, J.T. and Topole, K. (1992), "An efficient and robust algorithm for damage localization in offshore platforms", *Proceeding of the ASCE Tenth Structures Congress*, 543-546.

Wu, J.R. and Li, Q.S. (2004), "Finite element model updating for a high-rise structure based on ambient vibration measurements", *Eng. Struct.*, **26**, 979-990.

Yang, Y.B. and Chen, Y.J. (2009), "A new direct method for updating structural models based on measured modal data", *Eng. Struct.*, **31**, 32-42.

Yi, J.H. and Yun, C.B. (2004), "Comparative study on modal identification methods using output-only information", *Struct. Eng. Mech.*, **17**(3-4), 445-446.

Zhang, Q.W., Chang, C.C. and Chang, T.Y.P. (2000), "Finite element model updating for structures with parametric constraints", *Earthq. Eng. Struct. D.*, **29**(7), 927-944.

Zui, H., Shinke, T. and Namita, Y. (1996), "Practical formulas for estimation of cable tension by vibration method", *J. Struct. Eng. - ASCE*, **122**(6), 651-656.